Evaluation of Renal Perfusion: A Comparative Study between Intravoxel Incoherent Motion (IVIM) Imaging and Arterial Spin Labeling (ASL) to Assess Renal Blood Flow in Rodents

Ishimatsu, Keisuke
Advanced Imaging Research Center, University of Texas Southwestern Medical Center

Kikuchi, Kazufumi
Advanced Imaging Research Center, University of Texas Southwestern Medical Center

Moe, Orson W.
Charles and Jane Pak Center of Mineral Metabolism and Clinical Research, University of Texas Southwestern Medical Center

Oshio, Koichi
Department of Radiology, Juntendo University School of Medicine

他

出版情報：Magnetic Resonance in Medical Sciences. 24 (4), 2025. 日本磁気共鳴医学会
バージョン：

Magn Reson Med Sci 2025; 24: 2023-0169
doi:10.2463/mrms.mp.2023-0169 Published Online: December 4, 2024

MAJOR PAPER

Evaluation of Renal Perfusion: A Comparative Study between Intravoxel Incoherent Motion (IVIM) Imaging and Arterial Spin Labeling (ASL) to Assess Renal Blood Flow in Rodents

Keisuke Ishimatsu[1,2], Kazufumi Kikuchi[1,2], Orson W. Moe[3,4,5], Koichi Oshio[6], Kousei Ishigami[2], and Masaya Takahashi[1*]

Purpose: To compare diagnostic reliability between an intravoxel incoherent motion (IVIM) imaging and an arterial spin labeling (ASL) in assessment of renal blood flow in rodents.

Methods: We first evaluated 3 different fitting methods on 5 datasets of diffusion-weighted imaging (DWI) with 10 b-values (0–1000 s/mm^2) for bi-exponential analysis in IVIM imaging to calculate pseudo-diffusion parameters. Coefficient of variation (CV) for each parameter and correlation among the parameters was assessed to test the robustness of the 3 fitting methods. Subsequently, DWI and ASL methods were performed before and 14 days after onset of acute kidney injury (AKI) in a rat model. Temporal change before and after AKI onset in the pseudo-diffusion parameters in 3 fitting methods was compared with that in the renal blood flow (RBF) derived in the ASL method.

Results: The CVs in all IVIM parameters were the lowest in the fitting method that estimated pseudo-diffusion parameters after a fixed true-diffusion was determined where the pseudo- and true-diffusion coefficients had no correlation. The RBF substantially reduced (~50%, $P < 0.001$) due to the AKI onset; however, no pseudo-diffusion parameters in any of 3 fitting methods could not detect the change. Further, any pseudo-diffusion parameters showed no correlation with the RBF.

Conclusion: Pseudo-diffusion parameters in the IVIM concept were not reliable to estimate RBF in the study. Since the kidney has a unique profile in the "tissue flow", our data indicate that study design and interpretation of results needs to be carefully considered when IVIM imaging is used for evaluation of blood flow in tissue, especially in the kidney.

Keywords: *acute kidney injury, arterial spin labeling, bi-exponential model, intraintravoxel incoherent motion, renal perfusion*

[1]Advanced Imaging Research Center, University of Texas Southwestern Medical Center, Dallas, TX, USA
[2]Department of Clinical Radiology, Graduate School of Medical Sciences, Kyushu University, Fukuoka, Fukuoka, Japan
[3]Charles and Jane Pak Center of Mineral Metabolism and Clinical Research, University of Texas Southwestern Medical Center, Dallas, TX, USA
[4]Department of Internal Medicine, University of Texas Southwestern Medical Center, Dallas, TX, USA
[5]Department of Physiology, University of Texas Southwestern Medical Center, Dallas, TX, USA
[6]Department of Radiology, Juntendo University School of Medicine, Tokyo, Japan
*Corresponding author: Department of Radiological Technology/Radiology, Graduate School of Science/Medicine, Juntendo University, 2-1-1 Hongo, Bunkyo-ku, Tokyo 113-8421, Japan.
E-mail: m.takahashi.ic@juntendo.ac.jp

Received: December 22, 2023 | Accepted: November 12, 2024

Introduction

Diffusion weighted imaging (DWI) determines the apparent diffusion coefficient (ADC) which is a quantitative parameter that can be altered by pathophysiological changes.[1–5] Intravoxel incoherent motion (IVIM) concept based on the bi-exponential behavior[6] interprets that the fast components of ADC attribute to blood flow and microperfusion in the capillary network (pseudo-diffusion coefficient) and the latter to tissue microstructure (true-diffusion coefficient). These parameters are quantified as 'D*' and 'D', respectively, and the volume fraction of D* as 'f' in bi-exponential model as described below; however, there is still an argument if IVIM imaging is diagnostically useful.

In the kidney, Liang et al.[7] demonstrated that the measured D* and f correlated with the renal blood flow (RBF) measured by an arterial spin labeling (ASL) method in the

renal cortex before and after induction of acute kidney injury (AKI) in rats. They concluded that the IVIM imaging was an effective tool for assessing tissue perfusion. In contrast, Heusch et al.[8] found that the f correlated with the RBF while the D* did not. The authors described with citing a paper[9] that pseudo-diffusion parameters and ASL perfusions were not interchangeable and thus the diagnostic value of IVIM imaging was not clear.

The previous IVIM studies in the kidney were executed using different fitting methods for the bi-exponential model. For instance, Ren et al.[10] used 'full-fitting' method which calculate all IVIM parameters (D, D* and f) at once, whereas some other studies[7,8] used 'segmented-fitting' method which determine D first by mono-exponential fitting with higher b-values and then calculate D* and f with the fixed D. Although not in the kidney, a few studies investigate the effect in use of the different fitting methods in IVIM analysis on the reliability of the calculated 'tissue blood flow' values in the liver,[11] pancreas,[11] prostate[12] or breast.[13] The bi-exponential model requires nonlinear regression for parameter estimation. Although most of the investigators have executed by their own (home-made or commercially available) software, it is mathematically known that challenges include providing accurate initial parameter estimates to ensure convergence and obtaining parameter estimates with error intervals to account for experimental measurement errors.[14] Hence, it is worth investigating how the different fitting methods affect the estimated IVIM parameters and the variations, if any, might account for the discrepancies in evaluating diagnostic utility of IVIM in the results of previous studies.

The kidney has unique profile in the 'tissue flow' as it is one of the most vascularized organs and has the highest blood flow per unit tissue weight compared with the other organs (e.g. approximately 5 times higher than heart, 7 times higher than liver, and 8 times higher than brain).[15] In addition, the kidney has the urinary flow that may affect measure of the local 'perfusions'. Therefore, the conclusion in the different organs may not fit to the kidney. Thus, this physiological property respective to the principles of IVIM or ASL concepts the discrepancy in clinical utility of IVIM analysis might be caused.

The overall objective of this study was to evaluate the diagnostic utility of the IVIM imaging to assess blood flow in the kidney. We first compared the variability of the pseudo-diffusion parameters in different fitting models derived from identical data. For this purpose, we applied an identical set of measured DWI data into the IVIM analysis with 3 different fitting models that are commonly used for bi-exponential analysis in the IVIM concept. The dataset consists of 5 DWI with 10 b-values, which were obtained under the same physiological condition as possible to avoid any cause of the variation derived from variability of subjects. Second, we measured the pseudo-diffusion parameters by IVIM and compared with the results identified by ASL perfusions before and after the onset of AKI in a rat model to discuss the sensitivity and accuracy of the IVIM analysis for RBF.

Materials and Methods

Animal care

The protocols in this study were approved by Institutional Animal Care and Use Committee (IACUC) (approval number: #2008−0056). All animals received humane care during breeding, and all experiments were performed in accordance with relevant guidelines and regulations.[16]

MRI

All MRI studies were conducted in a 7.0T experimental horizontal system with a 35 mm inner diameter coil (Agilent, Palo Alto, CA, USA). To minimize motion artifacts, respiratory gating was performed with an MRI-compatible small-animal respiratory gating device (SA Instruments, Stony Brook, NY, USA).

Study I

We used a healthy male C57BL/6 mouse (12 week-old). Under anesthesia with 1.5%–2% isoflurane (AERRANE, Baxter Healthcare, IL, USA) mixed in 100% oxygen, the animal was placed supine with the abdomen centered with respect to the center of the RF coil. After localizer imaging was performed, coronal multislice T2-weighted images (T2WI) were obtained on both kidneys to identify the anatomy using a fast spin-echo sequence: TR/TE = 2500/40 ms, FOV = 32 × 32 mm, matrix size = 128 × 128, slice thickness = 1 mm, no intersection gap, fat suppression, number of excitation (NEX) = 4.

Since the purpose of Study I was to compare the variability derived only from the different fitting methods and not relating to subjects as much as possible, the 5 datasets were obtained intentionally in 1 animal under a consistent physiological condition (confirmed by monitoring the respiratory and cardiac rates). On a selected 1.5 mm coronal slice delineating both kidneys, a set of DW single shot echo-planar imaging (EPI) with 10 b-values (0, 50, 100, 200, 300, 400, 500, 600, 800, and 1000 s/mm^2 in random order) was conducted 5 times within ~20 mins. The other parameters were: TR/TE = 3000/38 ms, FOV = 32 × 32 mm, matrix size = 64 × 64, NEX = 1. The motion probing gradients (diffusion time = 16 ms, gradient pulse duration = 4 ms, gradient pulse separation = 17.3 ms) were applied concurrently on the 3 orthogonal directions.

Study II

Four rats (Sprague Dawley rat, 8 week-old) were subjected to the first MRI session (Pre) and then AKI was induced by single intraperitoneal injection of cisplatin (10 mg/kg; Sigma-Aldrich, St. Louis, MO, USA).[17] The same MRI

session was repeated at 14 days after injection (Post). Under anesthesia described above, coronal T2WI and a set of DW single shot EPI with the same imaging parameters in Study I except for the larger FOV (64 × 64 mm) and slice thickness (2.5 mm) were obtained. Subsequently, an ASL was performed to measure RBF in the same slice location using the flow-sensitive alternating inversion recovery (FAIR) technique.[18,19] A hyperbolic secant adiabatic pulse was used for inversion with 8 inversion times (TI = 250, 500, 1000, 1400, 1700, 2000, 3000, and 4000 ms). A selective inversion slice thickness of 6.5 mm was used to assure imaging slice thickness ratio of more than 2.5:1 to avoid artifacts from spins that are not fully inverted at the margins of the readout slice.[20] Single shot EPI was used for data acquisition with the following parameters: TR/TE = 10,000/38 ms, FOV = 64 × 64 mm, matrix size = 64 × 64, NEX = 1. For each TI, data were averaged from 10 pairs of control and labeled images. As the FAIR perfusion data were collected over a long period, to reduce errors in T_1 measurement, a T_1 mapping was also acquired using an inversion recovery spin echo EPI of the same imaging parameters but different TIs (31, 62, 125, 250, 500 1000, 2000, 4000, and 8000 ms) with 4 averages. Total scan time was approximately 90 mins.

Image Analysis

DWI data analysis

For DWI data analysis, the bi-exponential models are defined by the following equations:

$$S(b)/S(0) = f \times \exp(-b \times D^*) + (1 - f) \times \exp(-b \times D) \quad (1)$$

where S(0) corresponds to the signal intensity (SI) without diffusion weighting (b = 0) and S(b) is the SI acquired with different b-values. The IVIM parameters were defined as reported[6]: the pseudo-diffusion coefficient (D*; $\times 10^{-3}$ mm^2/s), volume fraction of pseudo-diffusion (f; %), and true-diffusion coefficient (D; $\times 10^{-3}$ mm^2/s). The product of f and D* (fD*) of which the value was suggested by Le Bihan and Turner[21] to show direct proportion to blood flow in the brain, was also calculated.

Fitting methods for IVIM analysis

We compared 3 different methods for the bi-exponential model (Eq. 1) on the DWI datasets in both studies via non-linear regression algorithm in a commercial software (Prism 5.0; GraphPad Software, La Jolla, CA, USA). These 3 methods are often used for the IVIM analysis in the recent reports as follows: Method-I; direct calculation of the 3 IVIM variables applying all 10 measured SIs at once, Method-II; direct calculation of the 3 IVIM variables using the measured SIs at only 6 b-values (0, 50, 100, 600, 800, and 1000 s/mm^2) excluding the b-values near the inflection point (200, 300, 400, and 500 s/mm^2), and Method-III; calculation of f and D* using all 10 b-values after a fixed true-diffusion coefficient, D, was determined.[22] To assess the appropriate fixed D for the Method-III, a mono-exponential fitting was applied to each diffusion dataset with 3 to 10 highest b-values in turn.

ASL quantification

For ASL quantification, the perfusion-weighted images were calculated by pairwise subtraction of the control and labeled images. To calculate RBF (ml/100 g/min), the perfusion-weighted signals at different TIs (ΔM(TI)) were fitted to the following kinetic function (Eq. 2) by a non-linear least-squares routine in Matlab (Mathworks, Natick, MA, USA)[23,24]:

$$\Delta M(TI) = 2M_0 \alpha F/\lambda \left[\frac{\exp(-TI/T_{1app}) - \exp(-TI/T_{1a})}{1/T_{1a} - 1/T_{1app}} \right] \quad (2)$$

where M_0 is the equilibrium magnetization, α is the inversion efficiency, F is the RBF (ml/100 g/min), λ is the blood-tissue partition coefficient, $1/T_{1app} = 1/T_1 + F/\lambda$ and T_{1a} is the longitudinal relaxation time of arterial blood. The M_0, α, and T_1 (the tissue longitudinal relaxation time) were determined from the 3-parameter fit of the T_1 mapping data. As previously reported, λ was set to 0.9 mL/g[25] and T_{1a} of 2210 ms was used.[26]

Other image analysis

In both Study I and II, the ROIs were manually placed on entire renal cortex avoiding partial volume effect. In DWI, SI was analyzed in air to provide an estimate of noise in each image and all measured SIs were corrected by the noise.[27] SNR was calculated as SI in the renal cortexes divided by SI in air. In Study I, IVIM parameters, f, D* and D, were derived from 3 different fitting methods on 5 DWI datasets obtained from the left kidney of the mouse. The coefficient of variation (CV) of IVIM parameters was assessed to test variability. In addition, the correlation between the D* and D in the 3 different fitting methods was tested. In Study II, the IVIM parameters derived from different methods and the RBF from ASL on all 8 kidneys were compared Pre and Post AKI. The correlation between each pseudo-diffusion parameter and the RBF at Pre and Post was also tested.

Statistical Analysis

All values are expressed as mean ± standard deviation (SD). The ADC in the renal cortex calculated from mono-exponential fitting using 3 to 10 (all) highest b-values were analyzed with Dunnett's multiple comparison test. RBF and IVIM parameters (f, D*, and D) from 3 different fitting methods between Pre and Post were compared with paired *t*-test. The correlation between D* and D (Study I) and between f, D* or fD*, and RBF were evaluated with a simple linear regression analysis. All statistical analyses

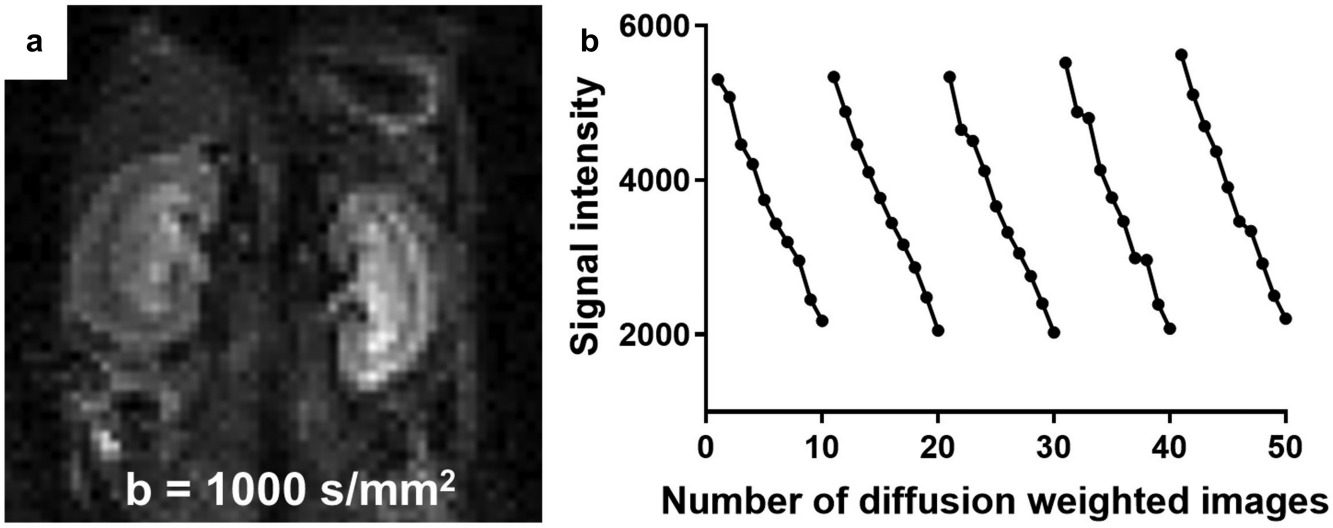

Fig. 1 (**a**) Representative coronal DWI at the highest b-value of 1000 s/mm^2. The SNR in the renal cortex was higher than 20. (**b**) The SIs in the left renal cortex in the 5 DWI datasets obtained in a normal healthy mouse within ~20 mins. The SIs for each b-value showed consistent decay over the datasets. DWI, diffusion weighted image; SI, signal intensity.

were performed by using a commercially available software (Prism 5.0), and $P < 0.05$ was considered to indicate a statistically significant difference.

Results

Study I

The temperature in the coil was kept at 28°C through the scan. The respiratory rate of the animal was almost consistent (35–38/min) during the DWI, affording that the effective TR for the respiratory gated DWI was 3.1–3.4 s in the all five datasets. When we placed the ROIs, there was no obvious position displacement in the kidney over the 50 images and the SNR in the renal cortexes on the DW images at the highest b-values of 1000 s/mm^2 was higher than 20 (22.1 $\pm$ 0.8) in the all 5 datasets (Fig. 1a). Figure 1b shows the SI over the b-values in the cortex of the left kidney through the five DWI datasets obtained in a normal healthy mouse within ~20 mins. The 5 SIs for each b-value were considered constant over the datasets in which the CV was <5%. The calculated true-diffusion in a mono-exponential fitting using the 3 b-values of higher than 600 s/mm^2 tended to increase according as it was calculated using the next lower b-value in turn (Fig. 2). Since it became significantly higher when using b-values lower than 300 s/mm^2, we used b-values of 400 s/mm^2 and above for the appropriate fixed true-diffusion (D) in the Method-III. Table 1 exhibits the f, D*, and D on the left kidney in the 3 different methods for the bi-exponential analysis. Method-III demonstrated the lowest variability in all calculated IVIM parameters. Further, the D* and D derived in the Methods-I and -II but -III demonstrated a significant correlation ($R^2 = 0.43$ and 0.31; Fig 3), implying that the D* and D might be calculated biased each other.

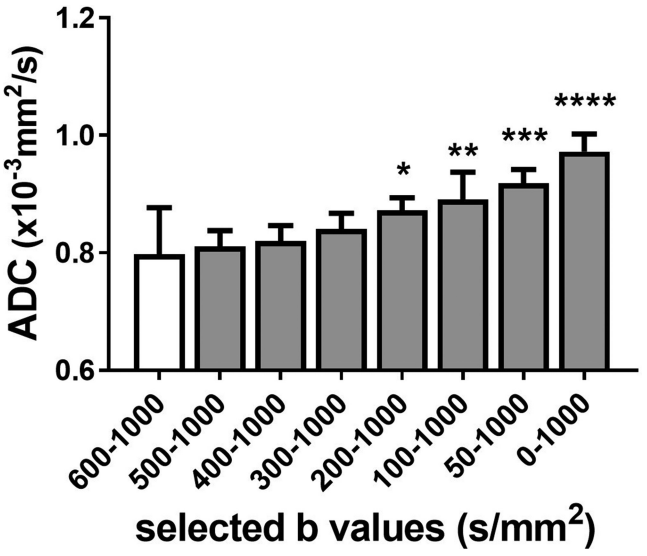

Fig. 2 ADC in the left renal cortex in a healthy normal mouse calculated from mono-exponential fitting using 3 to 10 (all) highest b-values. The ADC calculated using the highest 3 b-values (600, 800, and 1000 s/mm^2; open column) increased according as it was calculated using the next lower b-value (from left to right). Data are presented as mean $\pm$ standard deviation (SD). *: $P < 0.05$, **: $P < 0.01$, ***: $P < 0.001$, ****: $P < 0.0001$ vs. the ADC calculated using highest 3 b-values (600, 800 and 1000 s/mm^2; open column) by Dunnett's multiple comparison test. ADC, apparent diffusion coefficient.

Table 1 The IVIM parameters (f, D*, and D) in the left renal cortex calculated from all three fitting methods over the five diffusion datasets in a healthy normal mouse in *Study I*

	f (%)		D* ($\times 10^{-3}$mm^2/s)		D ($\times 10^{-3}$mm^2/s)		R square	
	Mean ± SD	CV (%)	Mean ± SD	CV (%)	Mean ± SD	CV (%)	Mean ± SD	CV (%)
Method-I	11.2 ±1.4	12.5	40.1 ± 61.1	152.3	0.850 ± 0.047	5.5	0.9963 ± 0.022	0.22
Method-II	21.7 ± 14.0	64.3	43.8 ± 81.7	186.6	0.720 ± 0.154	21.3	0.9984 ± 0.018	0.18
Method-III	12.3 ±1.5	12.2	11.9 ± 4.5	37.6	0.820 ± 0.026	3.2	0.9956 ± 0.021	0.21

CV, coefficient of variation; IVIM, intravoxel incoherent motion; SD, standard deviation.

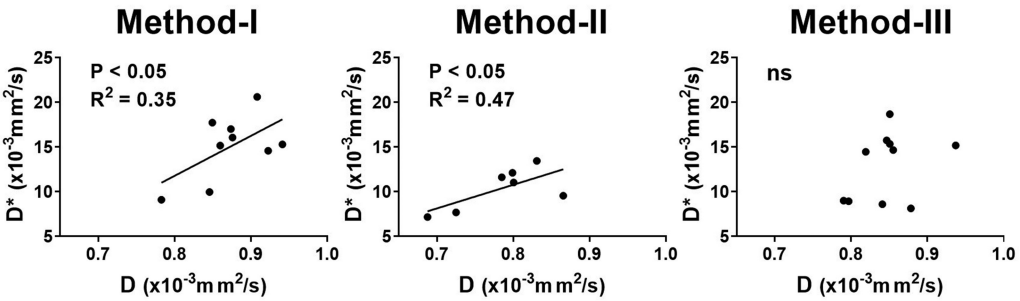

Fig. 3 Correlation between the D* and D in both kidneys in Study I. The D* and D derived from the Methods-I and -II demonstrated a significant correlation, implying that the D* and D might be calculated biased each other, while Method-III did not show correlation between the D* and D. The outliers (D* > 50×10^{-3} mm^2/s) were excluded.

Study II

Figure 4a shows the typical T2WIs and perfusion maps of Pre and Post. The SI in the outer stripe of outer medulla relatively increased compared to the cortex on T2WI. The RBF measured in both kidneys by the ASL significantly reduced after AKI onset (Pre: 249 ± 42 vs. Post: 126 ± 62 mL/100 g/min, $P < 0.001$; Fig. 4b). Any IVIM parameters did not show any significant differences between Pre and Post (Fig. 5). Further, there were no correlation between the RBF and the f, D* or fD* in all three methods (Fig. 6).

Discussion

Since the SI, respiratory frequency and temperature remained almost stable through the 5 sets of DWI scans (~20 mins) in the Study I, the physiological condition could be assumed as constant over the 5 datasets. Further, we obtained the 5 sets of DW images with 10 b-values in random order in each set so that the risk of temporal changes was averaged out. Hence, the variations in the results could be considered to relate the difference among the fitting methods. Further, the SNRs on all analyzed DW images were higher than 20. For these reasons, we believe that the 5 datasets were eligible for evaluation of variability to measure the IVIM parameters in all three fitting methods.

Mono-exponential analysis to determine an appropriate D for the Method-III demonstrated that the calculated ADC increased when using the b-values lower than 300 s/mm^2 because of inclusion of the perfusion effect as reported.[4] The D* in the kidney measured in the present study and other studies[7,28] were mostly higher than, at least, 10×10^{-3} mm^2/s. The total water signals from the component with the ADC of 10×10^{-3} mm^2/s at the b-value of 0 are calculated to decay at a rate of 92% and 98.2%, respectively, at b-values of 300 and 400 s/mm^2. Thus, it is reasonable to use b-values higher than ~300 s/mm^2 to measure true-diffusion separately from 'perfusion effect' in the kidney by mono-exponential analysis, which is a consistent conclusion in the previous studies.[4,29] In another word, we should use the b of higher than 300 s/mm^2 for assessing more precise cellularity in the tissue when apply mono-exponential model.

The smallest variation in the all IVIM parameters, f, D* and D, was provided in the Method-III. The Methods-I and -II exhibited extremely higher CV for D* and D. This caused by that 1 (Method-I) or 2 (Method-II) of 5 calculated data were extremely high. These outliers were derived from the bi-exponential fitting showing reasonable coefficient values (R^2; 0.9975, 0.9985 and 0.9987) which were not different from those in other data fittings (0.9937 ~ 0.9995). Both Park et al.[11] and Suo et al.[13] also compared different fitting methods for bi-exponential analysis including the 'full-fitting' and 'segmented-fitting' methods that are similar to our Method-I and Method-III in other organs. Their results indicated that the 'full-fitting' method had significantly

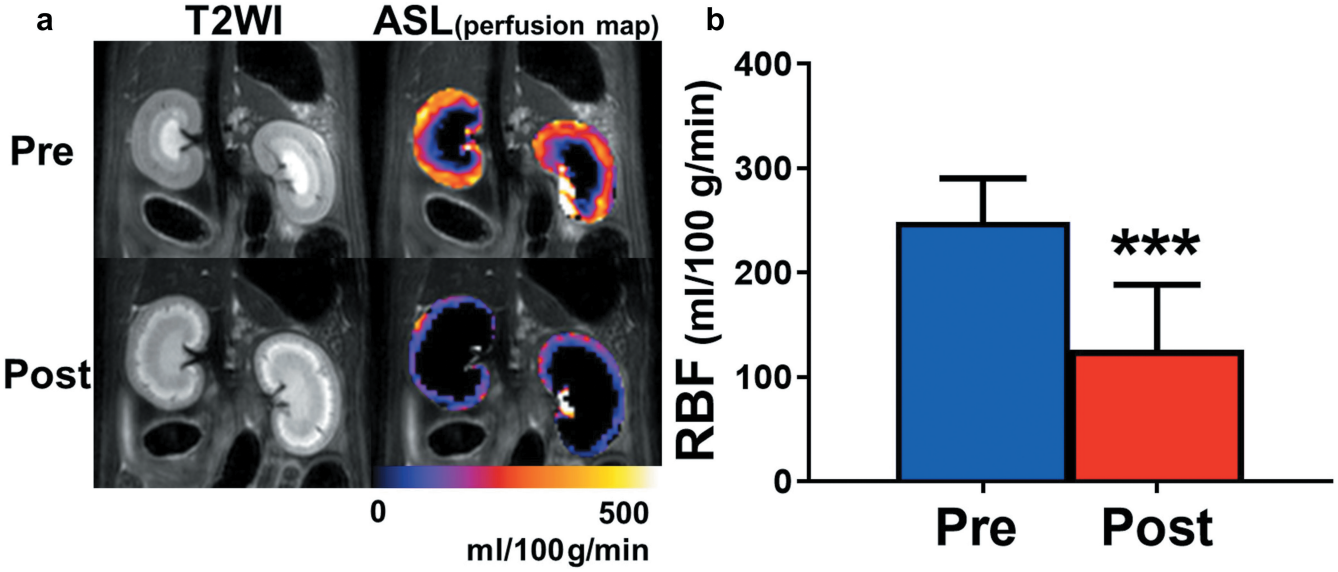

Fig. 4 (**a**) Typical T2WI and perfusion maps of before (Pre) and 14 days after (Post) onset of AKI in a rat model. Signal intensity in the outer stripe of outer medulla relatively increased compared to the cortex on T2WI and the renal perfusion reduced on the entire cortex after AKI onset. (**b**) The RBF of Pre and Post in the cortex measured by the ASL. ***: $P < 0.001$. AKI, acute kidney injury; ASL, arterial spin labelling; RBF, renal blood flow; T2WI, T2-weighted images.

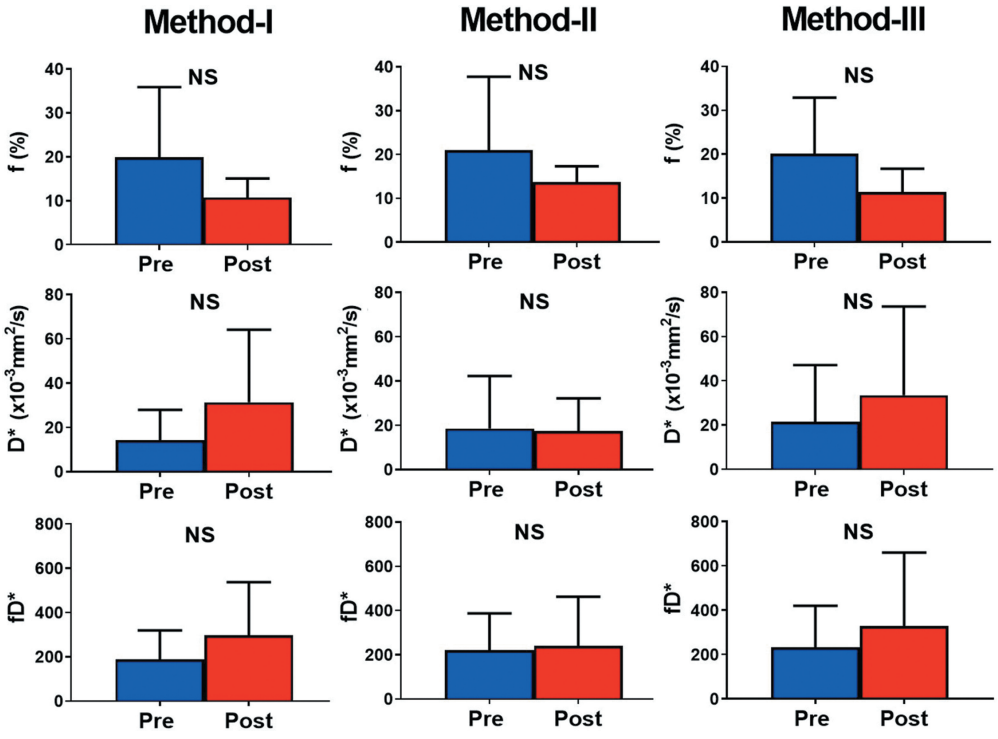

Fig. 5 The pseudo-diffusion parameters (f, D* and fD*) in the 3 fitting methods before (Pre) and 14 days after (Post) AKI onset in the renal cortex. AKI, acute kidney injury.

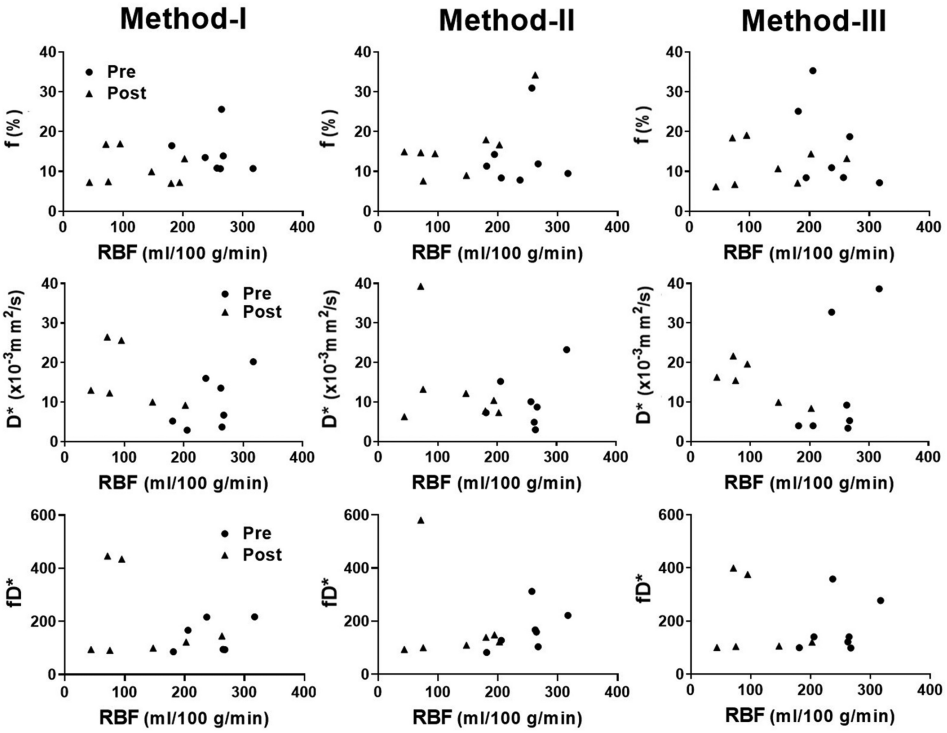

Fig. 6 The correlation between the RBF and pseudo-diffusion parameters (f, D* and fD*) in the 3 fitting methods in Study II. The outliers ($D^* > 50 \times 10^{-3}$ mm^2/s) were excluded. RBF, renal blood flow.

larger CVs for the f and/or D* and D than the 'segmented-fitting' method. Further, both studies reported the outliers in the 'full-fitting' method as observed in our study. The authors stated that the outliers might be caused due to a mathematical instability of the direct fitting for all 3 variables.[11,13] Our results also showed the close correlation between the D* and D in Methods-I and II although these parameters could be independent as indicated in the Method-III. The result might imply that these 2 parameters might have been calculated biased by each other in the Methods-I and -II and is an example for an error propagation from the measurements of the dependent variable to the parameter estimates.[14] Further, the D* ($14.9–16.7 \times 10^{-3}$ mm^2/s) and f (10.8%–18.0%) values in the renal cortex in previous reports[30,31] in the mouse kidney were closer to our values Method-III than Methods-I and II in this Study I. For all of these reasons, we concluded that the Method-III provided highest reliability for IVIM parameters among the 3 fitting methods in Study I.

In Study II, we used an established rat model of AKI induced by single injection of cisplatin.[17] In this model, the renal function measured by endogenous creatinine clearance to evaluate glomerular filtration rate deteriorates immediately after cisplatin injection and becomes the worst at 7 days but it recovers close to the normal level at 14 days. However, this recovery does not mean radical cure and the renal function would deteriorate again later.[32] The measured normal RBF value by the ASL at Pre was consistent with those in the previous studies,[33,34] which indicated that the measured RBF was reliable and could be the gold standard for blood flow. The ASL method clearly showed a substantial reduction (~50%) of RBF in the renal cortex at Post cisplatin-induced AKI. On the contrary, the f, D*, and fD* calculated in all Methods-I to -III could not detect the pathological reduction at Post. Further, neither f, D*,nor fD* correlated with the RBF identified by ASL. These results obviously demonstrated that the pseudo-diffusion parameters were not sensitive to detect the 50% reduction of RBF in the AKI model. Even Method-III, that reduces intrinsic mathematical instability and was the most reliable among three in Study I did not show a correlation with RBF, implying that evaluation of the renal blood flow via IVIM is limited.

A possible cause of the insensitive measure of RBF by the IVIM might refer to its unique physiological property of the kidney. First, the kidney involves both urinary and blood flow as stated above. ASL basically measures the change in SIs between with and without labeling the blood in the renal artery that goes into the kidney so that the signal change in the kidney is specific to the blood flow. In contrast, IVIM measures all the incoherent flowing/diffusing protons and thus is not able to differentiate blood flow from urinary flow. This fundamental issue affects more on the kidney than the other organs. Although the urinary volume was not measured in this study, to make matters worth, it is reported

that the urinary volume increased (approximately 2-folds) in a similar cisplatin-induced AKI rodent model 5 days after injection because of loss of urinary concentrating ability.[35,36] Therefore, the increased urinary flow, if any also in our study, must increase the pseudo-diffusion parameters and hide the reduction of the RBF whereas it did not affect the ASL measure. Another possible cause of the difference between the IVIM and ASL measurements may be the effect of cardiac cycle. Peak-systolic and end-diastolic velocities in the renal artery were 173 ± 51 cm/s and 40 ± 20 cm/s, respectively, in healthy human.[37] The pseudo-diffusion parameters might have been more affected by the variation in timing of excitation of the spin and acquisition of its signals over the large change (4-folds) in the velocity. By contrast, Kazan et al.[38] reported that the effect of cardiac cycle to the measured perfusion in the ASL is very small and negligible. Further, Henkelman[39] described that IVIM might be able to measure some properties of proton motion but it cannot measure perfusion since the unit of RBF was physiological (ml/100 g/min) which is different from that of pseudo-diffusion parameters D* (mm^2/s) and f (%) and thus does not seem to be comparable with RBF.

Nevertheless, there are, indeed, several studies showing the correlation between the pseudo-diffusion parameters and the RBF measured by the ASL in the kidney as describe above. One study[7] was conducted in the renal cortex in a rat model of AKI, which is similar to our study, but demonstrated the correlation between the f and D* with the RBF. In the study, for some reason, the RBF in the renal cortex in the normal rats (122.62 w ± 6.53 mL/100 g/min) was substantially lower than the results by our and other groups studies (240–360 mL/100 g/min),[33,34] which might have caused the difference. Another possible cause might be differences in the selection of b-values; they used 7 low (≤200 s/mm^2) b-values (0, 20, 40, 60, 80, 100, and 200 s/mm^2) whereas we used 4 low b-values (0, 50, 100, and 200 s/mm^2) although both studies used a total of 10 b-values. Hence, we analyzed the selection of the b-values in the previous reports, showing correlations between pseudo-diffusion parameters and the tissue blood flow although these studies investigated different species/organs (Table 2). The studies used 5–13 low b-values out of the total of 9–17 b-values.[7,8,40–47] Therefore, 4 low b-values might be too low to have any correlations in our study. However, Joo et al.[44] used 10 low b-values in the liver and no correlation was shown. Further, Bane et al.[40] used as many as 13 low b-values in the kidney and only the f correlated with the tissue blood flow. In addition, the pseudo-diffusion parameters correlated with the blood flow vary in each study. Recent studies described that the D was diagnostically useful than the D* and f in the renal dysfunction[48] or renal cancer.[49] For those reasons, we cannot conclude that the accuracy of the pseudo-diffusion increases as number of b-value increases and should note the numbers of b-value proportionally increase the total scan time. The appropriate number of b-values in IVIM imaging may vary depending upon the organ and/or the level of pathophysiological changes.

Variety of TEs used in the previous IVIM studies might be the other possible cause in evaluation of clinical utility of IVIM since it is known that the pseudo-diffusion parameters are TE-dependent.[50] Another study was reported[51] indicating that shorter diffusion time showed no significant changes in f and D*, although it tended to show a slight decrease in f. Shorter TE generally ensures higher signal intensity in the constant diffusion time leading to a more accurate estimated diffusion value and longer diffusion time increases restricted diffusion.[1] Jerome et al.[50] stated that the signal derived from flow components is enhanced with long TE because flow component has longer T2 and tissue component has shorter T2. The authors also demonstrated that the minimum TE provides close to the 'true f' and calculated f increases as TE becomes longer. The diffusion time (16 ms) and TE (38 ms) in the current study are presumed to be shorter or equivalent than those in the previous study (we estimated the diffusion time from the used TEs of 61–86 ms [Table 2] when it was not indicated in the manuscripts). It means that our estimated pseudo-diffusion parameters are closer to the real values than those in the previous studies but showed no correlations. Therefore, it is revealed that diffusion time/TE are not the sole determinant of no correlation between the pseudo-diffusion and RBF. Other imaging parameters (TR, pixel size, and slice thickness) in this study did not differ widely from those in previous studies,[7,8,40–47] indicating that they are unlikely to be major factors of the discrepancy with previous studies.

Conclusion

Even with the most reliable fitting method, the pseudo-diffusion parameters in the IVIM concept could not detect the reduced renal blood flow in the AKI model. The selection of b-values and bi-exponential fitting model and interpretation of the result need to be carefully considered when IVIM imaging is used for evaluation of tissue blood flow, especially in the kidney.

Acknowledgments

We thank Drs. Robert Lenkinski and Qing Yuan at the Department of Radiology, University of Texas Southwestern Medical Center, for helpful discussion.

Funding

This work was supported by NIH S10 OD023552 (M.T.), P41 EB015908 Shared Resource (Dr. Craig Malloy at UT Southwestern), R01 DK091392 and R01 DK092461 (O.W.M.), the O'Brien Kidney Research Center at UT Southwestern (P30 DK07938) (O.W.M.), the Pak Center Innovative Research Support, and Endowed Professors Collaborative Research Support (O.W.M.).

Table 2 Summary of previous studies reporting the correlation between the pseudo-diffusion parameters and the tissue perfusion.

Study	Pseudo-diffusion parameters correlated with perfusion	Technique for perfusion measurement	Organ	Species	# of total b-values	# of low b-values (≤ 200 s/mm^2)	Fitting method	TR/TE (ms)	Δ/δ (ms)	b-values (s/mm^2)
Our study	NA	ASL	Kidney	Rat	10	4	3 methods	3000/38	17.3/4	0, 50, 100, 200, 300, 400, 500, 600, 800, 1000
Heusch et al.[8]	f	ASL	Kidney	Human	16	5	Similar to Method-III	3000/75	NA	0, 50, 100, 150, 200, 250, 300, 350, 400, 450, 500, 550, 600, 650, 700, 750
Liang et al.[7]	f, D*, fD*	ASL	Kidney	Rat	10	7	Similar to Method-III	3000/73.6	NA	0, 20, 40, 60, 80, 100, 200, 400, 500, 600
Hu et al.[43]	f	ASL	Kidney	Rat	9	6	NA	2000/61	NA	0, 25, 50, 75, 100, 150, 300, 700, 1000
Bane et al.[40]	f	DCE	Kidney	Human	16	13	Bayesian algorithm	3000/74	NA	0, 15, 30, 45, 60, 75, 90, 105, 120, 135, 150, 175, 200, 400, 600, 800
Joo et al.[44]	NA	DCE	Liver tumor	Rabbit	12	10	Similar to Method-III	2700/63	NA	0, 10, 20, 30, 40, 50, 75, 100, 150, 200, 400, 800
Patel et al.[45]	NA	DCE	Liver	Human	9	5	Similar to Method-III	2000/86	NA	0, 50, 100, 150, 200, 300, 500, 700, 1000
Hectors et al.[42]	f, D*, fD*	DCE	Liver	Human	16	13	Bayesian algorithm	4500/74–81	NA	0, 15, 30, 45, 60, 75, 90, 105, 120, 135, 150, 175, 200, 400, 600, 800
Fujima et al.[41]	fD*	DCE	Head neck cancer	Human	12	8	Similar to Method-I and III	4500/64	30.1/24.3	0, 10, 20, 30, 50, 80, 100, 200, 400, 800, 1000, 2000
Yao et al.[47]	f, fD*	ASL	Brain	Human	16	8	Similar to Method-III	5200/minimum	NA	0, 20, 40, 80, 110, 140, 170, 200, 300, 400, 500, 600, 700, 800, 900, 1000
Shen et al.[46]	f, D*, fD*	ASL	Brain	Human	17	9	Similar to Method-III	5200/70.8	NA	0, 10, 20, 40, 80, 110, 140, 170, 200, 300, 400, 500, 600, 700, 800, 900, 1000

#, number; Δ, gradient pulse separation; δ, gradient pulse duration; ASL, arterial spin labeling; DCE, dynamic contrast-enhanced MRI

Conflicts of interest

The authors declare that they have no conflicts of interest.

References

1. Takahashi M, Hackney DB, Zhang G, et al. Magnetic resonance microimaging of intraaxonal water diffusion in live excised lamprey spinal cord. *Proc Natl Acad Sci USA* 2002; 99:16192–16196.
2. Togao O, Hiwatashi A, Yamashita K, et al. Differentiation of high-grade and low-grade diffuse gliomas by intravoxel incoherent motion MR imaging. *Neuro-oncol* 2016; 18:132–141.
3. Li H, Liang L, Li A, et al. Monoexponential, biexponential, and stretched exponential diffusion-weighted imaging models: Quantitative biomarkers for differentiating renal clear cell

carcinoma and minimal fat angiomyolipoma. *J Magn Reson Imaging* 2017; 46:240–247.
4. Togao O, Doi S, Kuro-o M, Masaki T, Yorioka N, Takahashi M. Assessment of renal fibrosis with diffusion-weighted MR imaging: Study with murine model of unilateral ureteral obstruction. *Radiology* 2010; 255:772–780.
5. Thoeny HC, Grenier N. Science to practice: Can diffusion-weighted MR imaging findings be used as biomarkers to monitor the progression of renal fibrosis? *Radiology* 2010; 255:667–668.
6. Le Bihan D, Breton E, Lallemand D, Aubin ML, Vignaud J, Laval-Jeantet M. Separation of diffusion and perfusion in intravoxel incoherent motion MR imaging. *Radiology* 1988; 168:497–505.
7. Liang L, Chen WB, Chan KW, et al. Using intravoxel incoherent motion MR imaging to study the renal pathophysiological process of contrast-induced acute kidney injury in rats: Comparison with conventional DWI and arterial spin labelling. *Eur Radiol* 2016; 26:1597–1605.
8. Heusch P, Wittsack HJ, Heusner T, et al. Correlation of biexponential diffusion parameters with arterial spin-labeling perfusion MRI: Results in transplanted kidneys. *Invest Radiol* 2013; 48:140–144.
9. Döpfert J, Lemke A, Weidner A, Schad LR. Investigation of prostate cancer using diffusion-weighted intravoxel incoherent motion imaging. *Magn Reson Imaging* 2011; 29:1053–1058.
10. Ren T, Wen CL, Chen LH, et al. Evaluation of renal allografts function early after transplantation using intravoxel incoherent motion and arterial spin labeling MRI. *Magn Reson Imaging* 2016; 34:908–914.
11. Park HJ, Sung YS, Lee SS, et al. Intravoxel incoherent motion diffusion-weighted MRI of the abdomen: The effect of fitting algorithms on the accuracy and reliability of the parameters. *J Magn Reson Imaging* 2017; 45:1637–1647.
12. Merisaari H, Movahedi P, Perez IM, et al. Fitting methods for intravoxel incoherent motion imaging of prostate cancer on region of interest level: Repeatability and gleason score prediction. *Magn Reson Med* 2017; 77:1249–1264.
13. Suo S, Lin N, Wang H, et al. Intravoxel incoherent motion diffusion-weighted MR imaging of breast cancer at 3.0 tesla: Comparison of different curve-fitting methods. *J Magn Reson Imaging* 2015; 42:362–370.
14. Lecca P, Lecca M, Maestri CA, Scarpa M. Biexponential fitting for noisy data with error propagation. *Math Methods Appl Sci* 2021; 44:10154–10171.
15. Verma SK, Molitoris BA. Renal endothelial injury and microvascular dysfunction in acute kidney injury. *Semin Nephrol* 2015; 35:96–107.
16. National Research Council (US) Committee for the Update of the Guide for the Care and Use of Laboratory Animals. Guide for the care and use of laboratory animals (8 ed.). Washington, DC:National Academies Press (US), 2011.
17. Panesso MC, Shi M, Cho HJ, et al. Klotho has dual protective effects on cisplatin-induced acute kidney injury. *Kidney Int* 2014; 85:855–870.
18. Kim SG. Quantification of relative cerebral blood flow change by flow-sensitive alternating inversion recovery (FAIR) technique: Application to functional mapping. *Magn Reson Med* 1995; 34:293–301.
19. Kwong KK, Chesler DA, Weisskoff RM, et al. MR perfusion studies with T1-weighted echo planar imaging. *Magn Reson Med* 1995; 34:878–887.
20. Karger N, Biederer J, Lusse S, et al. Quantitation of renal perfusion using arterial spin labeling with FAIR-UFLARE. *Magn Reson Imaging* 2000; 18:641–647.
21. Le Bihan D, Turner R. The capillary network: A link between IVIM and classical perfusion. *Magn Reson Med* 1992; 27:171–178.
22. Luciani A, Vignaud A, Cavet M, et al. Liver cirrhosis: Intravoxel incoherent motion MR imaging—pilot study. *Radiology* 2008; 249:891–899.
23. Pell GS, Thomas DL, Lythgoe MF, et al. Implementation of quantitative FAIR perfusion imaging with a short repetition time in time-course studies. *Magn Reson Med* 1999; 41:829–840.
24. Rajendran R, Lew SK, Yong CX, Tan J, Wang DJ, Chuang KH. Quantitative mouse renal perfusion using arterial spin labeling. *NMR Biomed* 2013; 26:1225–1232.
25. Herscovitch P, Raichle ME. What is the correct value for the brain—blood partition coefficient for water? *J Cereb Blood Flow Metab* 1985; 5:65–69.
26. Dobre MC, Ugurbil K, Marjanska M. Determination of blood longitudinal relaxation time (T1) at high magnetic field strengths. *Magn Reson Imaging* 2007; 25:733–735.
27. Miller AJ, Joseph PM. The use of power images to perform quantitative analysis on low SNR MR images. *Magn Reson Imaging* 1993; 11:1051–1056.
28. Jerome NP, Boult JK, Orton MR, et al. Modulation of renal oxygenation and perfusion in rat kidney monitored by quantitative diffusion and blood oxygen level dependent magnetic resonance imaging on a clinical 1.5T platform. *BMC Nephrol* 2016; 17:142.
29. Yamada I, Aung W, Himeno Y, Nakagawa T, Shibuya H. Diffusion coefficients in abdominal organs and hepatic lesions: Evaluation with intravoxel incoherent motion echo-planar MR imaging. *Radiology* 1999; 210:617–623.
30. Eberhardt C, Wurnig MC, Wirsching A, et al. Intravoxel incoherent motion analysis of abdominal organs: Computation of reference parameters in a large cohort of C57Bl/6 mice and correlation to microvessel density. *MAGMA* 2016; 29:751–763.
31. Hennedige T, Koh TS, Hartono S, et al. Intravoxel incoherent imaging of renal fibrosis induced in a murine model of unilateral ureteral obstruction. *Magn Reson Imaging* 2015; 33:1324–1328.
32. Shi M, McMillan KL, Wu J, et al. Cisplatin nephrotoxicity as a model of chronic kidney disease. *Lab Invest* 2018; 98:1105–1121.
33. Tan H, Thacker J, Franklin T, Prasad PV. Sensitivity of arterial spin labeling perfusion MRI to pharmacologically induced perfusion changes in rat kidneys. *J Magn Reson Imaging* 2015; 41:1124–1128.
34. Zimmer F, Zollner FG, Hoeger S, et al. Quantitative renal perfusion measurements in a rat model of acute kidney injury at 3T: Testing inter- and intramethodical significance of ASL and DCE-MRI. *PLoS One* 2013; 8:e53849.
35. Humanes B, Lazaro A, Camano S, et al. Cilastatin protects against cisplatin-induced nephrotoxicity without compromising its anticancer efficiency in rats. *Kidney Int* 2012; 82:652–663.

36. Moreno-Gordaliza E, Giesen C, Lazaro A, et al. Elemental bioimaging in kidney by LA-ICP-MS as a tool to study nephrotoxicity and renal protective strategies in cisplatin therapies. *Anal Chem* 2011; 83:7933–7940.
37. AbuRahma AF, Srivastava M, Mousa AY, et al. Critical analysis of renal duplex ultrasound parameters in detecting significant renal artery stenosis. *J Vasc Surg.* 2012; 56:1052-1060.e1.
38. Kazan SM, Chappell MA, Payne SJ. Modelling the effects of cardiac pulsations in arterial spin labelling. *Phys Med Biol* 2010; 55:799–816.
39. Henkelman RM. Does IVIM measure classical perfusion? *Magn Reson Med* 1990; 16:470–475.
40. Bane O, Wagner M, Zhang JL, et al. Assessment of renal function using intravoxel incoherent motion diffusion-weighted imaging and dynamic contrast-enhanced MRI. *J Magn Reson Imaging* 2016; 44:317–326.
41. Fujima N, Yoshida D, Sakashita T, et al. Intravoxel incoherent motion diffusion-weighted imaging in head and neck squamous cell carcinoma: Assessment of perfusion-related parameters compared to dynamic contrast-enhanced MRI. *Magn Reson Imaging* 2014; 32:1206–1213.
42. Hectors SJ, Wagner M, Besa C, et al. Intravoxel incoherent motion diffusion-weighted imaging of hepatocellular carcinoma: Is there a correlation with flow and perfusion metrics obtained with dynamic contrast-enhanced MRI? *J Magn Reson Imaging* 2016; 44:856–864.
43. Hu G, Yang Z, Liang W, et al. Intravoxel incoherent motion and arterial spin labeling MRI analysis of reversible unilateral ureteral obstruction in rats. *J Magn Reson Imaging* 2019; 50:288–296.
44. Joo I, Lee JM, Grimm R, Han JK, Choi BI. Monitoring vascular disrupting therapy in a rabbit liver tumor model: Relationship between tumor perfusion parameters at IVIM diffusion-weighted MR imaging and those at dynamic contrast-enhanced MR imaging. *Radiology* 2016; 278:104–113.
45. Patel J, Sigmund EE, Rusinek H, Oei M, Babb JS, Taouli B. Diagnosis of cirrhosis with intravoxel incoherent motion diffusion MRI and dynamic contrast-enhanced MRI alone and in combination: Preliminary experience. *J Magn Reson Imaging* 2010; 31:589–600.
46. Shen N, Zhao L, Jiang J, et al. Intravoxel incoherent motion diffusion-weighted imaging analysis of diffusion and microperfusion in grading gliomas and comparison with arterial spin labeling for evaluation of tumor perfusion. *J Magn Reson Imaging* 2016; 44:620–632.
47. Yao Y, Zhang S, Tang X, et al. Intravoxel incoherent motion diffusion-weighted imaging in stroke patients: Initial clinical experience. *Clin Radiol.* 2016; 71: 938.e11–938.e16.
48. Cheng ZY, Feng YZ, Hu JJ, et al. Intravoxel incoherent motion imaging of the kidney: The application in patients with hyperuricemia. *J Magn Reson Imaging* 2020; 51:833–840.
49. Ding Y, Tan Q, Mao W, et al. Differentiating between malignant and benign renal tumors: Do IVIM and diffusion kurtosis imaging perform better than DWI? *Eur Radiol* 2019; 29:6930–6939.
50. Jerome NP, d'Arcy JA, Feiweier T, et al. Extended T2-IVIM model for correction of TE dependence of pseudo-diffusion volume fraction in clinical diffusion-weighted magnetic resonance imaging. *Phys Med Biol* 2016; 61:N667.
51. Iima M, Nobashi T, Imai H, et al. Effects of diffusion time on non-Gaussian diffusion and intravoxel incoherent motion (IVIM) MRI parameters in breast cancer and hepatocellular carcinoma xenograft models. *Acta Radiol Open* 2018; 7:2058460117751565.